Chinese Chemical Letters 31 (2020) 2499–2502

Contents lists available at ScienceDirect

Chinese Chemical Letters

journal homepage: www.elsevier.com/locate/cclet

Communication

Enhanced photoluminescence and stability of ZnSe microspheres/Cs_4PbBr_6 microcrystals/$CsPbBr_3$ nanocrystals composites

Chao Zhang[a,b,c], Tingting Li[a,c], Lei Pu[a,c], Weijia Wen[a], Xiangdong Luo[b], Lijuan Zhao[a,c,*]

[a] Materials Genome Institute, Shanghai University, Shanghai 200444, China
[b] Jiangsu Key Laboratory of ASIC Design, Nantong University, Nantong 226019, China
[c] State Key Laboratory of Transducer Technology, Shanghai Institute of Microsystem and Information Technology, Chinese Academy of Sciences, Shanghai 200050, China

ARTICLE INFO

Article history:
Received 16 December 2019
Received in revised form 2 January 2020
Accepted 7 January 2020
Available online 9 January 2020

Keywords:
Dual-phase perovskites
Ternary complex
Supersaturated recrystallization
Photoluminescence
Passivation
Optoelectronic

ABSTRACT

A ternary complex combining dual-phase perovskites - $Cs_4PbBr_6/CsPbBr_3$ (DP-CPB) with ZnSe micropsheres (ZnSe-DP-CPB) was successfully prepared using supersaturated recrystallization technique at room temperature. It was showed that the DP-CPB composites were partially embedded in ZnSe microsphere composed with ZnSe NCs. The light absorption range of ZnSe-DP-CPB composites was extended from visible to near infrared light. Highly enhanced luminescence from ZnSe-DP-CPB composite was observed and the excitation power-dependent photoluminescence showed that the recombination involves excitons. The recombination lifetimes of the ternary composites increased compared with DP-CPB composite, indicating that the non-radiative combination was suppressed which may be possibly due to the decrease of both bulk and surface defects, owing to the passivation of ZnSe, as well as the suitable band alignments of these three components. The ternary complex also showed improved stability of photoluminescence (PL), which opens a new avenue for enhancing the stability of PL and optoelectronic applications for semiconductor-perovskite composites.

All-inorganic perovskite materials have attached much attention for their potential applications in the fields of light-emitting diodes (LEDs) [1], quantum dot displays [2], solar cells [3], photodetectors [4] and lasing [5]. Recent years, cesium lead halide perovskites have become one of the most widely-studied all-inorganic perovskite materials because of their attractive electrical and optical properties as well as excellent thermal stability [6]. Compared with traditional Cd-based II—VI semiconductor nanocrystals (NCs), all-inorganic cesium lead halide perovskites can be prepared by simple synthetic methods under ambient conditions [6–8]. For example, $CsPbBr_3$ nanocrystals (NCs), one of the most popular inorganic perovskite materials, can be synthesized in a large scale by supersaturated recrystallization (SR) technique at room temperature [8]. However, Cs_4PbBr_6 may be occurred in the synthesis of $CsPbBr_3$ NCs. Nevertheless, the PL intensity of mixture of Cs_4PbBr_6 and $CsPbBr_3$ was greatly enhanced compared with pure $CsPbBr_3$ [9]. Actually, in the past three years, Cs_4PbBr_6-related perovskite microcrystals (MCs) have drawn much attention because of strong green photoluminescence (PL) emission when the crystal's size changed from 1 μm to 1×10^4 μm. This strong green PL is not from pure Cs_4PbBr_6 MCs or NCs due to its large band gap (>3.90 eV) [10]. One truth is that it is difficult to prevent the occurrence of $CsPbBr_3$ in the synthesis of Cs_4PbBr_6 MCs [11]. Moreover it is confirmed that cubic-phase $CsPbBr_3$ can aligned with all three dimensions of Cs_4PbBr_6 lattice [12] and perovskite-related $CsPbBr_3/Cs_4PbBr_6$ MCs have improved stability and PL emission [13–15].

Recently, much effort has been made to study the combination of all-inorganic halide perovskite with other traditional semiconductor materials to improve their optical property and stability. Because of the good alignment of conduction band between metal oxides and inorganic halide perovskite, ZnO and TiO_2 have been introduced in perovskite-based devices [16–18]. As far as we know, there is no report on composites formed by perovskite NCs and other II—VI semiconductors. ZnSe is a typical II—VI semiconductor which has a wide direct band gap of 2.7 eV and a large exciton binding energy. And zinc-blende ZnSe has a lattice constant of 5.67 Å which is similar with that of $CsPbBr_3$ (5.83 Å). It is expected that perovskite NCs can align well with the lattice of ZnSe MCs. In this work, a ternary complex by combining the *in-situ* dual-phase Cs_4PbBr_6 MCs/$CsPbBr_3$ NCs (DP-CPB) composites with ZnSe

* Corresponding author at: Materials Genome Institute, Shanghai University, Shanghai 200444, China.
E-mail address: zhaolijuan@t.shu.edu.cn (L. Zhao).

https://doi.org/10.1016/j.cclet.2020.01.013
1001-8417/

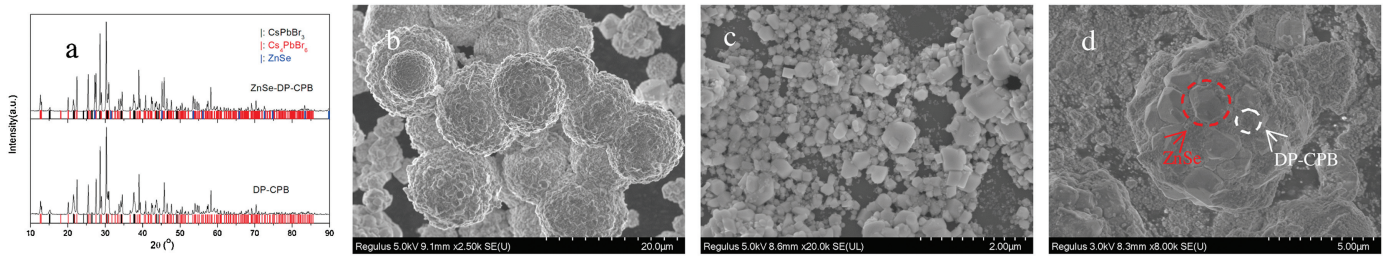

Fig. 1. (a) XRD patterns of DP-CPB and ZnSe-DP-CPB composites. SEM images of (b) ZnSe microspheres, (c) DP-CPB composites, (d) ZnSe-DP-CPB composites, respectively.

microspheres was prepared at room-temperature. The time-resolved PL (TRPL) of the ternary complex was measured and analyzed to throw light on the origin of enhanced PL. The results indicated that the ternary complex has longer PL lifetime and higher probability in radiation recombination. The good band alignment between perovskites and ZnSe as well as the passivation of ZnSe may be the possible reasons for the enhanced PL. The ternary composite also showed improving stability compared with DP-CPB composites. After stored at ambient environment of Shanghai in October for 33 days, the PL intensity of ternary complex remained up to 59%, whereas for the specimen without ZnSe, the remained PL intensity was less than 30%.

We used the reported procedure to prepare ZnSe microspheres [19]. The *in-situ* DP-CPB composites were synthesized by a supersaturated recrystallization (SR) process. The detailed preparations of ZnSe microspheres and DP-CPB composites were presented in Supporting information. ZnSe microspheres/Cs_4PbBr_6 MCs/$CsPbBr_3$ NCs (ZnSe-DP-CPB) composites were prepared by adding 0.4 mmol ZnSe microsphere powder to the DP-CPB composites precursor solution under magnetic stirring. Then, the mixture was quickly injected into 10 mL of toluene under violent magnetic stirring. After injection, strong glaring green emission can be observed. Finally, ZnSe-DP-CPB sample was precipitated from the solution by centrifugal separation. The morphology of the as-prepared samples was characterized by scanning electron microscope (SEM, HITACHI SU8230). Photoluminescence (PL) spectra were taken by a standard micro-area PL system with an excitation source of 405-nm continuous-wave laser. Time-resolved photoluminescence (TRPL) spectra were measured by a fluorescence lifetime imaging microscopy (FLIM) system based on time correlated single photo counting (TCSPC) technique with an excitation source of 200-ps laser pulses at 405 nm. Ultraviolet-visible (UV–vis) absorption spectra were measured by an UV–vis spectrophotometer (UV6500), equipped with an integrating sphere. X-ray diffraction (XRD) patterns were collected on a PANalytical Empyrean X-ray diffractometer with Cu target radiation source ($K\alpha$ =1.5406 Å), and the scanning angles (2θ) ranged from 10° to 90°.

The XRD patterns of DP-CPB and ZnSe-DP-CPB composites are depicted in Fig. 1a. The coexistence of $CsPbBr_3$ and Cs_4PbBr_6 can be observed in both the XRD patterns of DP-CPB and ZnSe-DP-CPB. The diffraction peaks at 15.1°, 15.2°, 21.5°, 26.5°, 30.4° and 34.5° are assigned to the (001), (100), (110), (−111), (002) and (−210) planes of monoclinic $CsPbBr_3$ (JCPDS No. 18-0364), respectively [20]. Strong diffraction peaks from highly crystallized rhombohedral Cs_4PbBr_6 (JCPDS No. 73-2478) are clearly demonstrated in Fig. 1a as well [21]. In the XRD spectrum of ZnSe-DP-CPB, diffraction peaks at 2θ = 27.2°, 45.2°, 83.4° and 89.8° which correspond to the (111), (220), (422) and (511) planes of cubic ZnSe (JCPDS No. 88-2345) are well resolved, which indicates that the ternary complex of DP-CPB with cubic ZnSe was formed. Figs. 1b-d show the SEM images of ZnSe, DP-CPB and ZnSe-DP-CPB, respectively. As shown in Fig. 1b, ZnSe microsphere comprised of large numbers of nanoparticles with an average size of 500−600 nm. The average diameter of ZnSe microspheres is about 8−10 μm. The SEM images of DP-CPB exhibit irregular morphology and small MCs at sub-micron scale size as shown in Fig. 1c. It can be clearly observed that these sub-micron MCs are surrounded by many rectangular grains with the size of 30–100 nm. Referring to the XRD results and the reported results [6], it is speculated that the irregular MCs are Cs_4PbBr_6, while the rectangular NCs are $CsPbBr_3$. As reported by Wang's group [6], Cs_4PbBr_6 MCs can act as a framework to provide a matrix for dispersing $CsPbBr_3$ NCs. It is believed that smaller sized $CsPbBr_3$ NCs are prone to be embedded into Cs_4PbBr_6 MCs during the reaction process, while larger $CsPbBr_3$ NCs are easy to precipitate. The sphere morphology was preserved well after the ternary complex of ZnSe-DP-CPB was formed and DP-CPB particles were found to be partially embedded into ZnSe micropsheres as depicted in Fig. 1d.

The elemental distributions were analyzed by selective-area energy disperse X-ray spectroscopy (EDS), and the corresponding elemental mappings indicate the uniform distributions of these five elements (Cs, Pb, Br, Zn and Se) in ZnSe-DP-CPB composites as shown in Fig. S1 (Supporting information), which further verified that DP-CPB composites were embedded in ZnSe micropshere. As shown in Figs. 2a and b, the atomic ratios of Cs, Pb and Br are found to be approximately 5.1:1.0:5.0 and 5.7:1.0:6.1 for DP-CPB and ZnSe-DP-CPB composites, respectively, suggesting that these products contain binary complex of Cs_4PbBr_6 and $CsPbBr_3$ [22]. The atomic ratio of Zn and Se was determined to be about 1.1:1.0 in EDX spectra of from ZnSe-DP-CPB composites (inset of Fig. 2b). All these EDS results are consistent well with the XRD results presented previously.

The optical properties of ZnSe-DP-CPB composite were investigated by room-temperature UV–vis absorption, steady PL and TRPL characterizations. Both DP-CPB and ZnSe-DP-CPB composites show two distinct absorption maxima located at 514 and 309 nm, corresponding to the interband transitions of $CsPbBr_3$ and Cs_4PbBr_6 [9], respectively, as indicated in the UV–vis absorption spectra shown in Fig. 3a. It is noted that a broad absorption shoulder centered at 678 nm was observed in the spectrum of ZnSe-DP-CPB composites, which is believed to be due to the transitions in ZnSe because no absorption was observed in

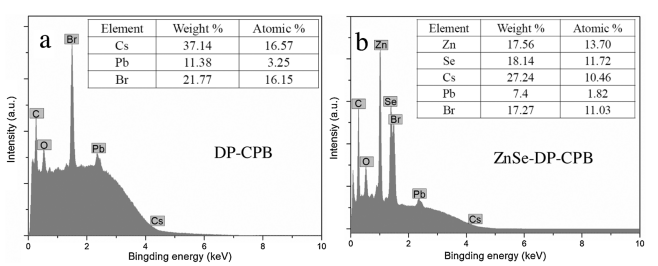

Fig. 2. Energy disperse spectrum (EDS) of (a) CP-CPB and (b) ZnSe-DP-CPB composites.

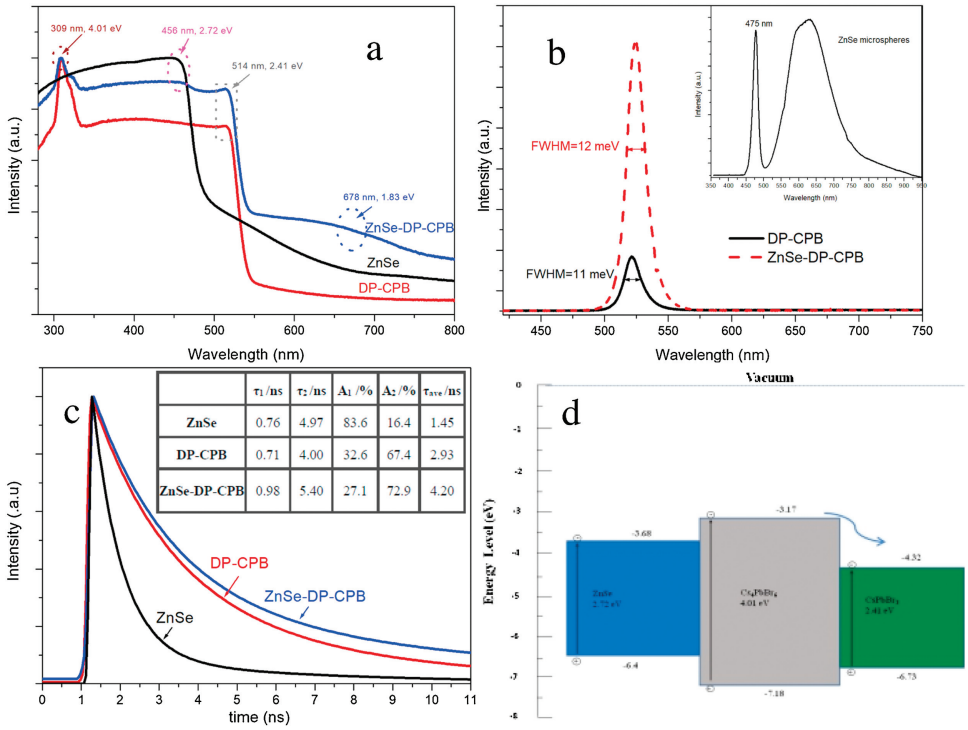

	τ_1/ns	τ_2/ns	A_1/%	A_2/%	τ_{ave}/ns
ZnSe	0.76	4.97	83.6	16.4	1.45
DP-CPB	0.71	4.00	32.6	67.4	2.93
ZnSe-DP-CPB	0.98	5.40	27.1	72.9	4.20

Fig. 3. (a) UV–vis absorption spectra of samples. (b) Steady PL spectra of DP-CPB and ZnSe-DP-CPB composites (inset is steady PL spectrum of ZnSe microspheres). (c) TRPL decay curves of samples. (d) Schematic band alignment of ZnSe-DP-CPB composite.

DP-CPB composite between 550 and 800 nm. Obviously, the absorption range of ZnSe-DP-CPB composite extended from visible to near infrared light. The band energies of $CsPbBr_3$ and Cs_4PbBr_6 are estimated to be around 2.41 eV and 4.01 eV, respectively. The absorption maximum of ZnSe microsphere was observed to be 456 nm which was assigned to the near-band-edge (NBE) absorption, corresponding to a band gap of 2.72 eV which has a small blue shift compared to bulk ZnSe material (2.67 eV) [23] due to the quantum confinement of small-size ZnSe grains.

Fig. 3b shows the steady PL spectra of DP-CPB and ZnSe-DP-CPB composites excited by a 405 nm of laser with the excitation power of 0.55 mW. DP-CPB composites exhibited strong PL emission at around 520 nm, which corresponds to the lowest absorption edge of $CsPbBr_3$ NCs. The PL spectrum of pure ZnSe microspheres is shown in the inset of Fig. 3b. As can be seen, peak in vicinity of 475 nm can be assigned to be the NBE emission from ZnSe, and the broad emission from 510 nm to 750 nm may come from the deep-defect related emission [24]. While in the PL of ZnSe-DP-CPB composite, neither NBE emission nor deep-defect related emission in ZnSe can be observed, indicating that the NBE emission of ZnSe is suppressed by the highly luminescence from $CsPbBr_3$ NCs and deep-level defects in ZnSe are greatly reduced after forming ZnSe-DP-CPB composite. It is observed as well that the PL intensity of ZnSe-DP-CPB composite was about 3.8 times higher than that of DP-CPB composite, which is probably due to the suppression of non-radiative recombination in $CsPbBr_3$ NCs by introducing ZnSe. The dependence of PL on excitation power was investigated to determine the nature of the recombination process [25] which is shown in Fig. S2 (Supporting information). The PL peak positions for both DP-CPB and ZnSe-DP-CPB composite samples did not change as excitation power increased. Insets in Fig. S2 show the pump-dependent PL intensity with slopes of 1.08 and 1.11 for these two samples, respectively, indicating that PL was originated from the single-photon excitation [26]. TRPL spectra of ZnSe, DP-CPB and ZnSe-DP-CPB composite are shown in Fig. 3c and all the decay curves can be fitted well by a biexponential function:

$$I(t) = A_1 e^{-\frac{t}{\tau_1}} + A_2 e^{-\frac{t}{\tau_2}} \quad (1)$$

where τ_1 and τ_2 are the lifetimes of short and long-lived PL components, A_1 and A_2 represent the amplitudes of the corresponding lifetimes, respectively. The biexponential decays demonstrate that two different species are involved in the exciton recombination. The average lifetime τ_{ave} is calculated by an expression $(A_1\tau_1^2 + A_2\tau_2^2)/(A_1\tau_1 + A_2\tau_2)$ and the fitting parameters are shown in the inset of Fig. 3e. For ZnSe microsphere, DP- CPB and ZnSe-DP-CPB composite, the decay fitting gives short lifetimes of τ_1 = 0.76, 0.71 and 0.98 ns which may be associated with trap-assisted recombination at grain boundaries or surfaces and long lifetimes of τ_2 = 4.97, 4.00 and 5.40 ns which may be related to radiative recombination inside the grains, respectively [27,28].

Generally, the amplitude A_1 of τ_1 decreased from ZnSe microsphere to ZnSe-DP-CPB composite, while A_2 of τ_2 increased. ZnSe-DP-CPB composites had longer lifetimes in both short and long-lived PL components compared with DP-CPB composite, indicative of less bulk and surface defects which is possibly due to ZnSe-induced surface passivation [29]. The average lifetime τ_{ave} is determined to be 1.45, 2.93 and 4.20 ns for ZnSe microsphere, DP-CPB and ZnSe-DP-CPB composite, respectively. It was noted that ZnSe-DP-CPB composite has a marginally slower average lifetime, indicating that trap-assisted recombination decreased after introduction of ZnSe. The stronger PL from ZnSe-DP-CPB composites reveals the high ratios of radiative-to-nonradiative transition in this ternary complex. Combining the above analyses, the possible energy band diagram of the ternary composite ZnSe-DP-CPB is proposed and shown in Fig. 3d. The valence-band-maxima differences between ZnSe, Cs_4PbBr_6 and $CsPbBr_3$ are referred to the previous reports [22,30]. Taking Cs_4PbBr_6 as axis of symmetry, type-I heterojunctions are formed between $CsPbBr_3$ and Cs_4PbBr_6, ZnSe and Cs_4PbBr_6, respectively. The photo-generated electrons in conduction band of Cs_4PbBr_6 prefer to transfer to the conduction

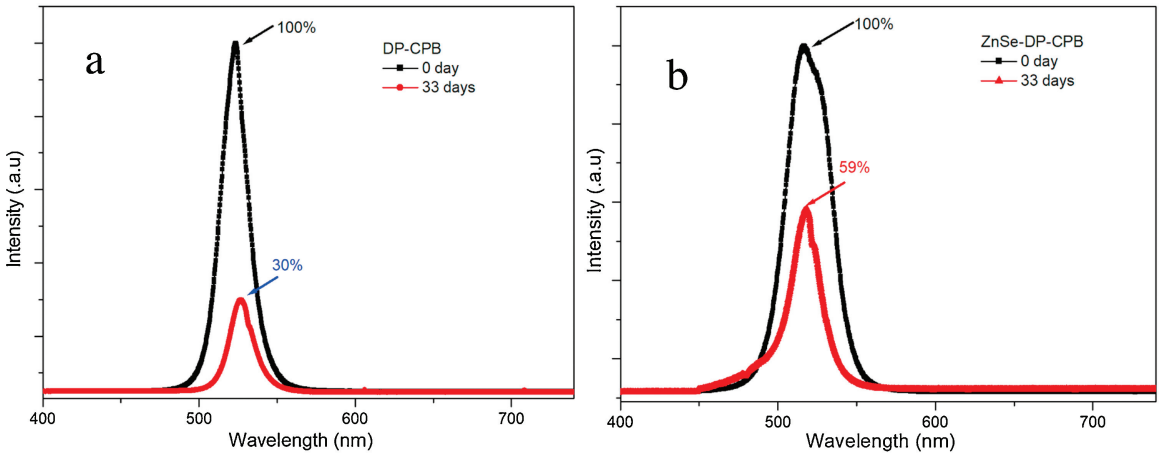

Fig. 4. The decrease of PL intensity of (a) DP-CPB and (b) ZnSe-DP-CPB composites stored in ambient environment for 33 days.

band of $CsPbBr_3$ which locates at lower energy. Meanwhile holes left in valence band of Cs_4PbBr_6 would transfer to the valence band of ZnSe and $CsPbBr_3$ due to type-I band alignment. Therefore, the enhanced PL emission from the ternary composite can be caused by the following three possible reasons: (1) Type-I energy alignment between $CsPbBr_3$ and Cs_4PbBr_6, resulting in a high carrier concentration and recombination rate in $CsPbBr_3$ NCs; (2) Improved near-band-edge emission from ZnSe due to the passivation of deep-level defects; (3) Enhanced radiative recombination in $CsPbBr_3$ NCs due to ZnSe-induced surface passivation. Since the ternary complex earned the enhanced PL partially owing to the less defect concentration, it is expected that the ternary complex would have enhanced stability of PL, which is further supported by the time-dependent PL measurement described below.

The stability of PL is studied by measuring the time-dependent PL spectra of DP-CPB and ZnSe-DP-CPB composites stored in an ambient environment without any protection. As shown in Fig. 4a, the PL intensity of DP-CPB composite reduced to 30% after being stored in ambient environment of Shanghai in October (temperature ~ 25 °C, relative humidity ~ 70%) for 33 days (Fig. 4a). For the ternary complex ZnSe-DP-CPB, the PL intensity reduced to 59% after being stored for 33 days, which can be attributed to the PL quenching of $CsPbBr_3$ on the surface of composite [22] as shown in Fig. 4b. Obviously, the stability of PL for the ternary complex ZnSe-DP-CPB is improved over that of DP-CPB composites. Therefore, it is believed that the improved stability of PL for ZnSe-DP-CPB composite can be attributed to the passivation effect of ZnSe which can protect $CsPbBr_3$ NCs from the erosion of moisture and oxygen. The improvement of ZnSe-passivation for PL stability of DP-CPB has promise for beneficial application in LED field.

In summary, a ternary complex of ZnSe-DP-CPB combining dual-phase Cs_4PbBr_6 MCs/$CsPbBr_3$ NCs composites with ZnSe microspheres was successfully prepared at room temperature. SEM images showed that the DP-CPB composites were partially embedded in ZnSe microsphere composed with ZnSe NCs. ZnSe-DP-CPB composite showed an extensional absorption from visible to near infrared light and enhanced PL emission. TRPL results reveal that ZnSe-DP-CPB composite has a longer lifetime, which indicates the reduction of both surface and bulk defects due to the ZnSe-passivation effect as well as the improvement of rediative recombination due to the suitable band alignment between these three components. The measurements on stability of PL showed that ZnSe-DP-CPB composites possess higher stability of PL than pure $CsPbBr_3$ NCs and ZnSe-$CsPbBr_3$ composites, which proves the passivation of Cs_4PbBr_6 and ZnSe. We believe these results would open a new avenue for great potential studying semiconductor-perovskite composites as highly luminescent emitters in optoelectronic applications and enhancing the stability of PL for perovskite materials.

Declaration of competing interest

The authors would like to declare that there is no conflict of interest existing in the submission of this manuscript.

Acknowledgments

This work is supported by National Natural Science Foundation of China (Nos. 61927806, 61474067) and the State Key Laboratory of Transducer Technology of China (No. SKT1806).

Appendix A. Supplementary data

Supplementary material related to this article can be found, in the online version, at doi:https://doi.org/10.1016/j.cclet.2020.01.013.

References

[1] J. Song, J. Li, X. Li, et al., Adv. Mater. 27 (2015) 7162–7167.
[2] H.C. Wang, S.Y. Lin, A.C. Tang, et al., Angew. Chem. Int. Ed. 55 (2016) 7924–7929.
[3] R.J. Sutton, G.E. Eperon, L. Miranda, et al., Adv. Energy Mater. 6 (2016) 1502458.
[4] Y. Dong, Y. Gu, Y. Zou, et al., Small 12 (2016) 5622–5632.
[5] Y. Fu, H. Zhu, C.C. Stoumpos, et al., ACS Nano 10 (2016) 7963–7972.
[6] Q. Wang, W. Wu, R. Wu, et al., J. Colloid Interfaces Sci. 554 (2019) 133–141.
[7] D. Chen, Z. Wan, X. Chen, et al., J. Mater. Chem. C 4 (2016) 10646–10653.
[8] X. Li, Y. Wu, S. Zhang, et al., Adv. Funct. Mater. 26 (2016) 2435–2445.
[9] Q.A. Akkerman, S. Park, E. Radicci, et al., Nano Lett. 17 (2017) 1924–1930.
[10] M. Nikl, E. Mihokova, K. Nitsch, et al., Chem. Phys. Lett. 306 (1999) 280–284.
[11] W. Wang, D. Wang, F. Fang, et al., Cryst. Growth Des. 18 (2018) 6133–6141.
[12] L.N. Quan, R. Quintero-Bermudez, O. Voznyy, et al., Adv. Mater. 29 (2017) 1605945–1605950.
[13] X. Chen, F. Zhang, Y. Ge, et al., Adv. Funct. Mater. 28 (2018) 1706567–1706573.
[14] Y. Wang, D. Yu, Z. Wang, et al., Small 13 (2017) 1701587–1701594.
[15] J.H. Cha, J.H. Han, W. Yin, et al., J. Phys. Chem. Lett. 8 (2017) 565–570.
[16] Y. Jiang, J. Liao, Y. Xu, et al., J. Mater. Chem. A 7 (2019) 13762–13769.
[17] D. Yang, R. Yang, J. Zhang, et al., Energy Environ. Sci. 8 (2015) 3208–3214.
[18] D. Son, B.J. Moon, A. Lee, et al., Appl. Surf. Sci. 483 (2019) 165–169.
[19] L. Zhao, C. Sun, G. Tian, Q. Pang, J. Colloid Inter. Sci. 502 (2017) 1–7.
[20] J. Zhang, L. Fan, J. Li, et al., Nano Res. 12 (2019) 121–127.
[21] P. Uthirakumar, M. Devendiranb, J.H. Parka, et al., Prog. Org. Coat. 132 (2019) 1–8.
[22] G. Hu, W. Qin, M. Liu, et al., J. Mater. Chem. C 7 (2019) 4733–4739.
[23] B. Feng, J. Cao, J. Yang, et al., Appl. Phys. A 118 (2015) 563–568.
[24] B. Feng, J. Cao, J. Yang, et al., Mater. Res. Bull. 60 (2014) 794–801.
[25] F. Luckert, M.V. Yakushev, C. Faugeras, et al., J. Appl. Phys. 111 (2012) 093507.
[26] W. Wu, S. Ren, Q. Han, et al., Phys. Chem. Chem. Phys. 20 (2018) 23556–23563.
[27] H. Cho, S.H. Jeong, M.H. Park, et al., Science 350 (2015) 1222–1225.
[28] H. Lu, Y. Tang, L. Rao, et al., Nanotechnology 30 (2019) 295603.
[29] Q. Chen, H. Zhou, T.B. Song, et al., Nano Lett. 14 (2014) 4158–4163.
[30] R. Marschall, Adv. Funct. Mater. 24 (2014) 2421–2440.